

Supporting Information

1. Frequency-dependent specific capacitance of the P-doped SiO₂ nanogranular proton-conducting film and the origin of the anticlockwise hysteresis loop on the transfer curve for the SiO₂ proton conductor gated oxide-based synaptic transistor.

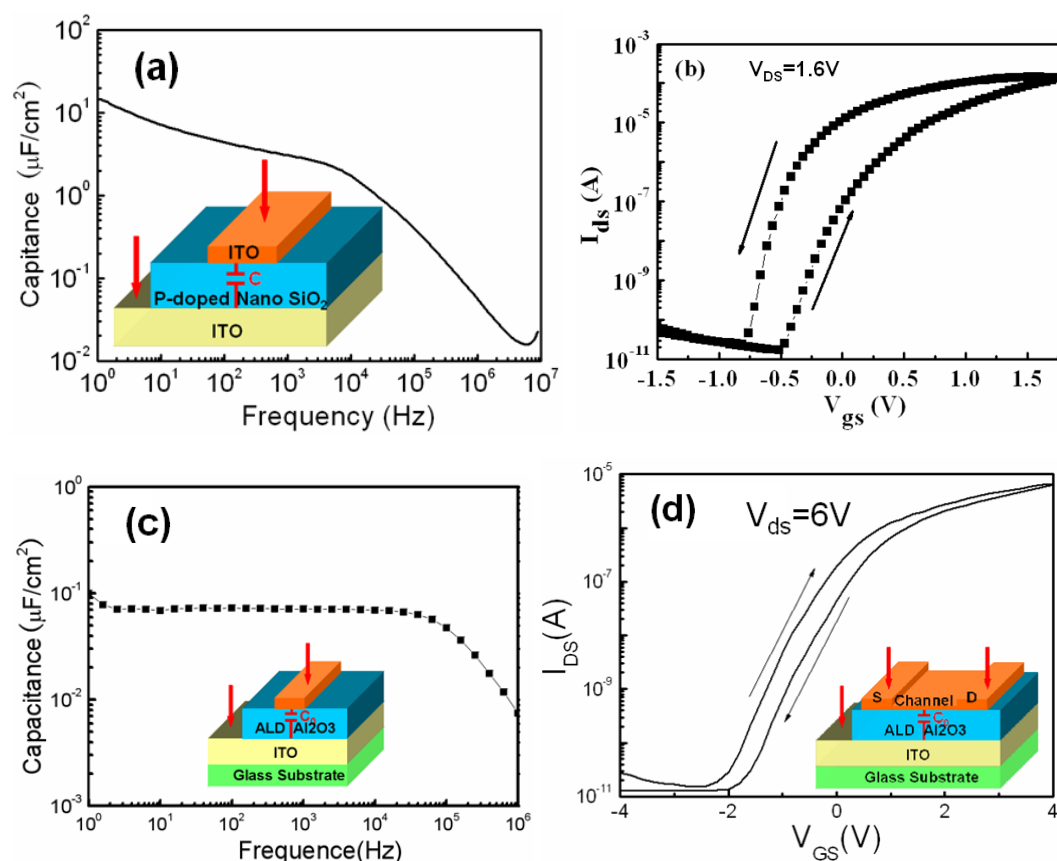


Figure S1 (a) Frequency-dependent specific capacitance of the P-doped SiO₂ nanogranular electrolyte film. (b) The transfer curve of the IZO-based synaptic transistors measured at $V_{\text{DS}}=1.6$ V. (c) The specific capacitance-frequency curves of the Al₂O₃ film deposited by atomic layer deposition (ALD) method. (d) The transfer curve for IZO TFTs gated by 60 nm Al₂O₃ dielectric deposited by ALD at $V_{\text{DS}}=6.0$ V, and a small clockwise hysteresis loop is obtained due to the existence of negative charge in the Al₂O₃ film.

The frequency-dependent capacitances of the P-doped nanogranular SiO₂ film and the Al₂O₃ dielectric film deposited by atomic layer deposition are obtained by the Solartron 1260 impedance analyzer. Figure S1 (a) illustrates frequency-dependent

specific capacitance of the P-doped SiO₂ nanogranular proton conducting film. A high specific capacitance of ~15 μF/cm² at 1.0 Hz is obtained due to the proton migration induced electric-double-layer (EDL) effect at the ITO/P-doped SiO₂ interface. Figure S1 (b) illustrates the transfer curve of the oxide-based synaptic transistor measured at the V_{ds} of 1.6V. A large anticlockwise hysteresis loop is obtained.

To clarify origins of the hysteresis loop in I_{ds}-V_{gs} curves, we also fabricated IZO thin-films transistor gated by Al₂O₃ dielectrics deposited by atomic layer deposition method for comparison. Figure S1(c) illustrate the capacitance-frequency curves for the Al₂O₃ films with the thickness of ~60 nm. The maximum specific capacitance of ~0.1 μF/cm² is obtained at 1.0 Hz. Much lower than that for the nanogranular SiO₂ films (~15 μF/cm²). Figure S1 (d) illustrates the transfer curve for IZO TFTs gated by atomic layer deposited Al₂O₃ dielectric films. A small clockwise hysteresis loop is obtained due to the existence of negative charge in the Al₂O₃ film. So the main reason for the large anticlockwise hysteresis loop is due to the mobile protons in nanogranular SiO₂ proton conductor [1, 2].

2. Transfer curves of the oxide-based synaptic transistor before and after a forming process.

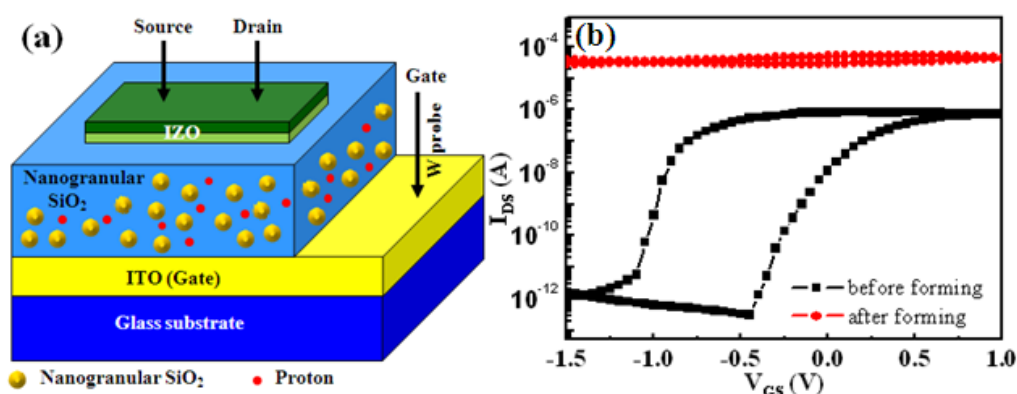


Figure S2 (a) The schematic picture of the oxide-based synaptic transistor. (b) The transfer curves (I_{DS} vs V_{GS}) of the synaptic transistor with V_{ds}=0.2 V: before and after a forming process.

Figure S2 (a) shows the schematic picture of the oxide-based synaptic transistor. Figure S2 (b) shows the transfer characteristics (I_{ds} vs V_{gs}) of the IZO synaptic transistor before and after a forming process. The forming process is performed by applying 4 V bias on the gate for 20 s. Before the process, the device performs as typical n-type field-effect transistors (the black line). After the process, drain current (I_{DS}) of the device keeps high and can not be tuned by altering the gate voltage (red line), indicating that a persistent high conduction is obtained as a result of the irreversible electrochemical process at the IZO/P-doped SiO_2 interface.

3. IZO channel conductance decay curves stimulated by different gate pulse numbers.

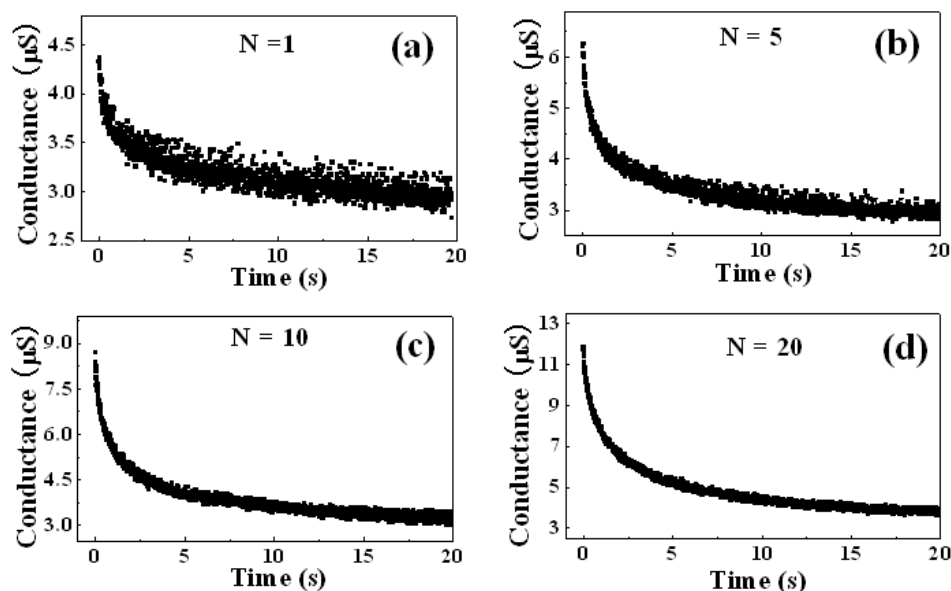


Figure S3 IZO channel conductance decay curves stimulated by different gate pulse numbers. Gate pulse: 1.0 V, 100 ms.

Figure S3 (a)-(d) shows the channel conductance decay curves with V_{DS} of 0.1V in air ambient by applying a series number (N=1, 5, 10, 20) of input gate pulses (1.0 V, 100 ms). Both of the cases, the conductance progressively increase by the applied gate pulses and rapidly decays back to a static equilibrium value of $\sim 3 \mu\text{S}$. The conductance changes agree well with a stretched exponential function: [3, 4]

$$G = (G_0 - G_\infty) \exp[-(t/\tau)^\beta] + G_\infty$$

where τ is the relaxation time, G_0 is the peak value of the triggered channel conductance, G_∞ is the final value of decay conductance, and β is the stretch index ranging between 0 and 1.

4. The relative humidity (RH) dependent electric-double-layer capacitance of the ITO/SiO₂/ITO sandwich structure.

Figure R4 shows the humidity dependent specific capacitance of the P-doped SiO₂ electrolyte film. The results show that the EDL capacitance increases with increased RH. Figure R5 shows the transfer curve and leakage current curve in vacuum (RH: 0%). No drain current modulation is observed in vacuum. So our results indicate that certain humidity is necessary for the EDL transistor and artificial synapse mimicking. Such discussion has been included in our revised manuscript and the Supporting Information.

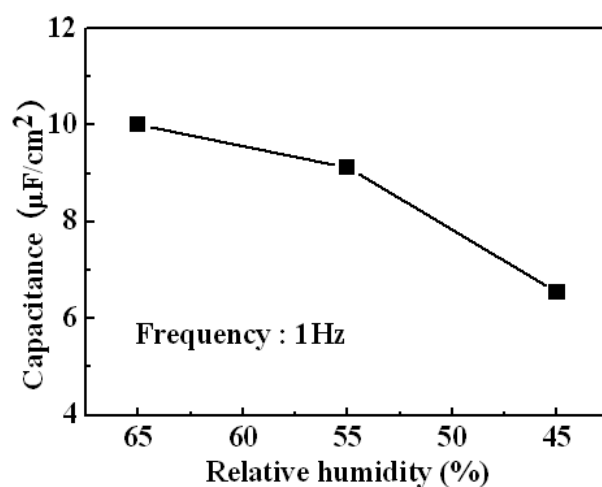


Figure R4. Relative humidity dependent specific capacitance values of of the P-doped SiO₂ electrolyte film.

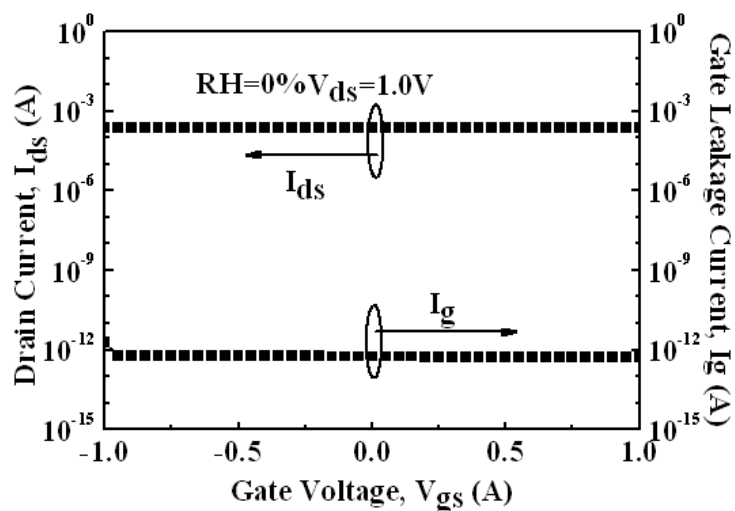


Figure R5. Transfer curve (up) and leakage current (bottom) curve of the synaptic transistor under vacuum (RH: 0%).

Reference

- [1] J. Yoon, W. K. Hong, M. Jo, G. Jo, M. Choe, P. Wark, J. I. Sohn, N Sedic, H. Hwang, M. E. Welland, T. Lee, *ACS Nano*. **2010**, 5, 558.;
- [2] H. T. Yuan, H. Shimotani, A. Tsukazaki, A. Ohtomo, M. Kawasaki, Y. Iwasa, *J. Am. Chem. Soc.*, **2010**, 132, 6672-6678;
- [3] B. Sturman, E. Podivilov, *Physical Review Letters*. **2003**, 91, 176602;
- [4] T.Chang, J S. Ho, W.Lu, *ACS Nano*, **2011**,5, 7669.